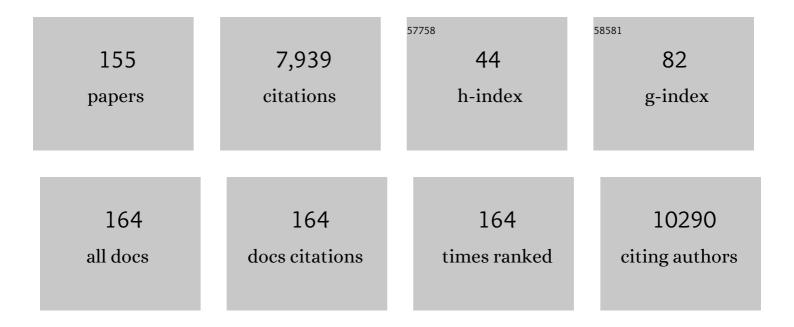
List of Publications by Year in descending order

Source: https://exaly.com/author-pdf/1090887/publications.pdf Version: 2024-02-01



700 lie Lui

#	Article	IF	CITATIONS
1	Structural insights into the activation of chemokine receptor CXCR2. FEBS Journal, 2022, 289, 386-393.	4.7	7
2	MD Simulations Revealing Special Activation Mechanism of Cannabinoid Receptor 1. Frontiers in Molecular Biosciences, 2022, 9, 860035.	3.5	4
3	Molecular insights into ligand recognition and G protein coupling of the neuromodulatory orphan receptor GPR139. Cell Research, 2022, 32, 210-213.	12.0	13
4	Structural insights into the activation initiation of full-length mGlu1. Protein and Cell, 2021, 12, 662-667.	11.0	19
5	Cryo-EM analysis of the HCoV-229E spike glycoprotein reveals dynamic prefusion conformational changes. Nature Communications, 2021, 12, 141.	12.8	17
6	Novel Functionalized Cannabinoid Receptor Probes: Development of Exceptionally Potent Agonists. Journal of Medicinal Chemistry, 2021, 64, 3870-3884.	6.4	8
7	Inhibition mechanism of SARS-CoV-2 main protease by ebselen and its derivatives. Nature Communications, 2021, 12, 3061.	12.8	149
8	Protocol for crystal structure determination of the antagonist-bound human cannabinoid receptor CB2. STAR Protocols, 2021, 2, 100584.	1.2	1
9	Rational Remodeling of Atypical Scaffolds for the Design of Photoswitchable Cannabinoid Receptor Tools. Journal of Medicinal Chemistry, 2021, 64, 13752-13765.	6.4	9
10	A Genetically Encoded F-19 NMR Probe Reveals the Allosteric Modulation Mechanism of Cannabinoid Receptor 1. Journal of the American Chemical Society, 2021, 143, 16320-16325.	13.7	44
11	Carbon-silicon switch led to the discovery of novel synthetic cannabinoids with therapeutic effects in a mouse model of multiple sclerosis. European Journal of Medicinal Chemistry, 2021, 226, 113878.	5.5	2
12	Crystal structure of semisynthetic obelinâ $\epsilon$ •v. Protein Science, 2021, , .	7.6	4
13	Organized cannabinoid receptor distribution in neurons revealed by super-resolution fluorescence imaging. Nature Communications, 2020, 11, 5699.	12.8	18
14	Structural and Functional Insights into Cannabinoid Receptors. Trends in Pharmacological Sciences, 2020, 41, 665-677.	8.7	40
15	Structural basis of CXC chemokine receptor 2 activation and signalling. Nature, 2020, 585, 135-140.	27.8	128
16	Structural features of activated GPCR signaling complexes. Current Opinion in Structural Biology, 2020, 63, 82-89.	5.7	50
17	A Novel G Protein-Biased and Subtype-Selective Agonist for a G Protein-Coupled Receptor Discovered from Screening Herbal Extracts. ACS Central Science, 2020, 6, 213-225.	11.3	25
18	Activation and Signaling Mechanism Revealed by Cannabinoid Receptor-Gi Complex Structures. Cell, 2020, 180, 655-665.e18.	28.9	212

#	Article	IF	CITATIONS
19	The structural study of mutation-induced inactivation of human muscarinic receptor M4. IUCrJ, 2020, 7, 294-305.	2.2	9
20	Disulfideâ€Containing Detergents (DCDs) for the Structural Biology of Membrane Proteins. Chemistry - A European Journal, 2019, 25, 11635-11640.	3.3	5
21	Probing the CB <sub>1</sub> Cannabinoid Receptor Binding Pocket with AM6538, a High-Affinity Irreversible Antagonist. Molecular Pharmacology, 2019, 96, 619-628.	2.3	4
22	Functionalityâ€Independent DNA Encoding of Complex Natural Products. Angewandte Chemie - International Edition, 2019, 58, 9254-9261.	13.8	54
23	A Chemical Strategy for Amphiphile Replacement in Membrane Protein Research. Langmuir, 2019, 35, 4319-4327.	3.5	6
24	Molecular Mechanism for Ligand Recognition and Subtype Selectivity of α2C Adrenergic Receptor. Cell Reports, 2019, 29, 2936-2943.e4.	6.4	17
25	Elucidating the active δ-opioid receptor crystal structure with peptide and small-molecule agonists. Science Advances, 2019, 5, eaax9115.	10.3	81
26	Structural Basis of the Diversity of Adrenergic Receptors. Cell Reports, 2019, 29, 2929-2935.e4.	6.4	30
27	Crystal Structure of the Human Cannabinoid Receptor CB2. Cell, 2019, 176, 459-467.e13.	28.9	268
28	Self-capping of nucleoprotein filaments protects the Newcastle disease virus genome. ELife, 2019, 8, .	6.0	18
29	Common activation mechanism of class A GPCRs. ELife, 2019, 8, .	6.0	339
30	High-throughput identification of G protein-coupled receptor modulators through affinity mass spectrometry screening. Chemical Science, 2018, 9, 3192-3199.	7.4	33
31	5-HT2C Receptor Structures Reveal the Structural Basis of GPCR Polypharmacology. Cell, 2018, 172, 719-730.e14.	28.9	185
32	Identification of natural products as novel ligands for the human 5-HT2C receptor. Biophysics Reports, 2018, 4, 50-61.	0.8	23
33	Protein crystal quality oriented disulfide bond engineering. Protein and Cell, 2018, 9, 659-663.	11.0	14
34	Computational design of thermostabilizing point mutations for G protein-coupled receptors. ELife, 2018, 7, .	6.0	60
35	Exploring a new ligand binding site of G protein-coupled receptors. Chemical Science, 2018, 9, 6480-6489.	7.4	37
36	Crystal Structure of ATP-Bound Human ABCF1 Demonstrates a Unique Conformation of ABC Proteins. Structure, 2018, 26, 1259-1265.e3.	3.3	14

#	Article	IF	CITATIONS
37	Structural and functional analyses of human DDX41 DEAD domain. Protein and Cell, 2017, 8, 72-76.	11.0	20
38	Human GLP-1 receptor transmembrane domain structure in complex with allosteric modulators. Nature, 2017, 546, 312-315.	27.8	192
39	Ligand identification of the adenosine A <sub>2A</sub> receptor in self-assembled nanodiscs by affinity mass spectrometry. Analytical Methods, 2017, 9, 5851-5858.	2.7	7
40	Crystal structures of agonist-bound human cannabinoid receptor CB1. Nature, 2017, 547, 468-471.	27.8	379
41	Structure and Function of a C–C Bond Cleaving Oxygenase in Atypical Angucycline Biosynthesis. ACS Chemical Biology, 2017, 12, 142-152.	3.4	17
42	The emerging roles of the DDX41 protein in immunity and diseases. Protein and Cell, 2017, 8, 83-89.	11.0	72
43	Biochemical features of the adhesion G protein-coupled receptor CD97 related to its auto-proteolysis and HeLa cell attachment activities. Acta Pharmacologica Sinica, 2017, 38, 56-68.	6.1	6
44	Mitrocomin from the jellyfish Mitrocoma cellularia with deleted C-terminal tyrosine reveals a higher bioluminescence activity compared to wild type photoprotein. Journal of Photochemistry and Photobiology B: Biology, 2016, 162, 286-297.	3.8	18
45	Crystal structure of hGEF-H1 PH domain provides insight into incapability in phosphoinositide binding. Biochemical and Biophysical Research Communications, 2016, 471, 621-627.	2.1	2
46	In vitro expression and analysis of the 826 human G protein-coupled receptors. Protein and Cell, 2016, 7, 325-337.	11.0	53
47	Native phasing of x-ray free-electron laser data for a G protein–coupled receptor. Science Advances, 2016, 2, e1600292.	10.3	97
48	Crystal Structure of the Human Cannabinoid Receptor CB1. Cell, 2016, 167, 750-762.e14.	28.9	468
49	Structural basis for DNA recognition by STAT6. Proceedings of the National Academy of Sciences of the United States of America, 2016, 113, 13015-13020.	7.1	46
50	aKMT Catalyzes Extensive Protein Lysine Methylation in the Hyperthermophilic Archaeon Sulfolobus islandicus but is Dispensable for the Growth of the Organism. Molecular and Cellular Proteomics, 2016, 15, 2908-2923.	3.8	16
51	All Ca2+-binding loops of light-sensitive ctenophore photoprotein berovin bind magnesium ions: The spatial structure of Mg2+-loaded apo-berovin. Journal of Photochemistry and Photobiology B: Biology, 2016, 154, 57-66.	3.8	16
52	New insights into the structural basis of DNA recognition by HINa and HINb domains of IF116. Journal of Molecular Cell Biology, 2016, 8, 51-61.	3.3	48
53	Combination Therapy of LysGH15 and Apigenin as a New Strategy for Treating Pneumonia Caused by Staphylococcus aureus. Applied and Environmental Microbiology, 2016, 82, 87-94.	3.1	51
54	A primase subunit essential for efficient primer synthesis by an archaeal eukaryotic-type primase. Nature Communications, 2015, 6, 7300.	12.8	18

#	Article	IF	CITATIONS
55	Structures of the Ca <sup>2+</sup> -regulated photoprotein obelin Y138F mutant before and after bioluminescence support the catalytic function of a water molecule in the reaction. Acta Crystallographica Section D: Biological Crystallography, 2014, 70, 720-732.	2.5	23
56	Structural and Biochemical Characterization Reveals LysGH15 as an Unprecedented "EF-Hand-Like― Calcium-Binding Phage Lysin. PLoS Pathogens, 2014, 10, e1004109.	4.7	85
57	Crystal structure of the Nâ€ŧerminal methyltransferaseâ€like domain of anamorsin. Proteins: Structure, Function and Bioinformatics, 2014, 82, 1066-1071.	2.6	12
58	Crystal structures of the F88Y obelin mutant before and after bioluminescence provide molecular insight into spectral tuning among hydromedusan photoproteins. FEBS Journal, 2014, 281, 1432-1445.	4.7	26
59	Structural and functional analyses of human tryptophan 2,3-dioxygenase. Proteins: Structure, Function and Bioinformatics, 2014, 82, 3210-3216.	2.6	46
60	Crystallization, preliminary X-ray crystallographic and cryo-electron microscopy analysis of a bifunctional enzyme fucokinase/ <scp>L</scp> -fucose-1-P-guanylyltransferase from <i>Bacteroides fragilis</i> . Acta Crystallographica Section F, Structural Biology Communications, 2014, 70, 1206-1210.	0.8	2
61	NLRC3, a Member of the NLR Family of Proteins, Is a Negative Regulator of Innate Immune Signaling Induced by the DNA Sensor STING. Immunity, 2014, 40, 329-341.	14.3	245
62	Role of the HIN Domain in Regulation of Innate Immune Responses. Molecular and Cellular Biology, 2014, 34, 2-15.	2.3	36
63	Mechanism of the Rpn13-induced activation of Uch37. Protein and Cell, 2014, 5, 616-630.	11.0	27
64	Structural analysis of asparaginyl endopeptidase reveals the activation mechanism and a reversible intermediate maturation stage. Cell Research, 2014, 24, 344-358.	12.0	86
65	Binding of bacterial secondary messenger molecule c di-GMP is a STING operation. Protein and Cell, 2013, 4, 117-129.	11.0	18
66	Spatial structure of the novel light-sensitive photoprotein berovin from the ctenophore Beroe abyssicola in the Ca2+-loaded apoprotein conformation state. Biochimica Et Biophysica Acta - Proteins and Proteomics, 2013, 1834, 2139-2146.	2.3	25
67	Structural biology study of human TNF receptor associated factor 4 TRAF domain. Protein and Cell, 2013, 4, 687-694.	11.0	17
68	Oxygen Activation of Apoâ€obelin–Coelenterazine Complex. ChemBioChem, 2013, 14, 739-745.	2.6	31
69	Structural basis for termination of AIM2-mediated signaling by p202. Cell Research, 2013, 23, 855-858.	12.0	38
70	Structure of the Leanyer orthobunyavirus nucleoprotein-RNA complex reveals unique architecture for RNA encapsidation. Proceedings of the National Academy of Sciences of the United States of America, 2013, 110, 9054-9059.	7.1	59
71	Structure of Severe Fever with Thrombocytopenia Syndrome Virus Nucleocapsid Protein in Complex with Suramin Reveals Therapeutic Potential. Journal of Virology, 2013, 87, 6829-6839.	3.4	67
72	High-resolution crystal structure of the catalytic domain of human dual-specificity phosphatase 26. Acta Crystallographica Section D: Biological Crystallography, 2013, 69, 1160-1170.	2.5	10

Zнı-Jie Liu

#	Article	IF	CITATIONS
73	Studies of Human 2,4-Dienoyl CoA Reductase Shed New Light on Peroxisomal $\hat{l}^2$ -Oxidation of Unsaturated Fatty Acids. Journal of Biological Chemistry, 2012, 287, 28956-28965.	3.4	17
74	The helicase DDX41 recognizes the bacterial secondary messengers cyclic di-GMP and cyclic di-AMP to activate a type I interferon immune response. Nature Immunology, 2012, 13, 1155-1161.	14.5	363
75	Structural View of a Non Pfam Singleton and Crystal Packing Analysis. PLoS ONE, 2012, 7, e31673.	2.5	2
76	Structural Analysis of the STING Adaptor Protein Reveals a Hydrophobic Dimer Interface and Mode of Cyclic di-GMP Binding. Immunity, 2012, 36, 1073-1086.	14.3	282
77	Structural insights into a human anti-IFN antibody exerting therapeutic potential for systemic lupus erythematosus. Journal of Molecular Medicine, 2012, 90, 837-846.	3.9	25
78	S-SAD phasing study of death receptor 6 and its solution conformation revealed by SAXS. Acta Crystallographica Section D: Biological Crystallography, 2012, 68, 521-530.	2.5	24
79	Structural and functional characterization of the C-terminal catalytic domain of SSV1 integrase. Acta Crystallographica Section D: Biological Crystallography, 2012, 68, 659-670.	2.5	13
80	Conversion of <scp>d</scp> â€ribulose 5â€phosphate to <scp>D</scp> â€xylulose 5â€phosphate: new insights from structural and biochemical studies on human RPE. FASEB Journal, 2011, 25, 497-504.	0.5	28
81	Protein-protein complexation in bioluminescence. Protein and Cell, 2011, 2, 957-972.	11.0	20
82	A multi-dataset data-collection strategy produces better diffraction data. Acta Crystallographica Section A: Foundations and Advances, 2011, 67, 544-549.	0.3	25
83	Altered architecture of substrate binding region defines the unique specificity of UDPâ€GalNAc 4â€epimerases. Protein Science, 2011, 20, 856-866.	7.6	14
84	Crystal structure of a novel non-Pfam protein PF2046 solved using low resolution B-factor sharpening and multi-crystal averaging methods. Protein and Cell, 2010, 1, 453-458.	11.0	13
85	Sequence fingerprint and structural analysis of the SCOR enzyme A3DFK9 from <i>Clostridium thermocellum</i> . Proteins: Structure, Function and Bioinformatics, 2010, 78, 603-613.	2.6	1
86	Structureâ€function analysis of human lâ€prostaglandin D synthase bound with fatty acid molecules. FASEB Journal, 2010, 24, 4668-4677.	0.5	1
87	NMR-derived Topology of a GFP-photoprotein Energy Transfer Complex*. Journal of Biological Chemistry, 2010, 285, 40891-40900.	3.4	47
88	Structure-function analysis of human l-prostaglandin D synthase bound with fatty acid molecules. FASEB Journal, 2010, 24, 4668-4677.	0.5	40
89	Structural Basis and Catalytic Mechanism for the Dual Functional Endo-β-N-Acetylglucosaminidase A. PLoS ONE, 2009, 4, e4658.	2.5	52
90	Structural insight into acute intermittent porphyria. FASEB Journal, 2009, 23, 396-404.	0.5	45

Zнı-Jie Liu

#	Article	IF	CITATIONS
91	Crystal structure of human esterase D: a potential genetic marker of retinoblastoma. FASEB Journal, 2009, 23, 1441-1446.	0.5	31
92	Structural Basis for the Inhibition of Human 5,10-Methenyltetrahydrofolate Synthetase by N10-Substituted Folate Analogues. Cancer Research, 2009, 69, 7294-7301.	0.9	16
93	Structure based mechanism of the Ca <sup>2+</sup> â€induced release of coelenterazine from the <i>Renilla</i> binding protein. Proteins: Structure, Function and Bioinformatics, 2009, 74, 583-593.	2.6	19
94	Novel dimerization mode of the human Bcl-2 family protein Bak, a mitochondrial apoptosis regulator. Journal of Structural Biology, 2009, 166, 32-37.	2.8	46
95	Structure of acostatin, a dimeric disintegrin from Southern copperhead ( <i>Agkistrodon contortrix) Tj ETQq1 1 2008, 64, 466-470.</i>	0.784314 2.5	rgBT /Overlo 20
96	Purification, crystallization and preliminary crystallographic analysis of the non-Pfam protein AF1514 fromArcheoglobus fulgidusDSM 4304. Acta Crystallographica Section F: Structural Biology Communications, 2008, 64, 91-93.	0.7	0
97	Crystal structure solution of a ParBâ€like nuclease at atomic resolution. Proteins: Structure, Function and Bioinformatics, 2008, 70, 263-267.	2.6	7
98	Crystal structure of a novel nonâ€Pfam protein AF1514 from <i>Archeoglobus fulgidus</i> DSM 4304 solved by Sâ€6AD using a Cr Xâ€ray source. Proteins: Structure, Function and Bioinformatics, 2008, 71, 2109-2113.	2.6	8
99	Crystal structure of coelenterazine-binding protein from Renilla muelleri at 1.7 Ã: Why it is not a calcium-regulated photoprotein. Photochemical and Photobiological Sciences, 2008, 7, 442.	2.9	31
100	The First Agmatine/Cadaverine Aminopropyl Transferase: Biochemical and Structural Characterization of an Enzyme Involved in Polyamine Biosynthesis in the Hyperthermophilic Archaeon Pyrococcus furiosus. Journal of Bacteriology, 2007, 189, 6057-6067.	2.2	31
101	Crystal structure of an aerobic FMN-dependent azoreductase (AzoA) from Enterococcus faecalis. Archives of Biochemistry and Biophysics, 2007, 463, 68-77.	3.0	66
102	Curved EFC/F-BAR-Domain Dimers Are Joined End to End into a Filament for Membrane Invagination in Endocytosis. Cell, 2007, 129, 761-772.	28.9	366
103	Structure of dNTP-inducible dNTP triphosphohydrolase: insight into broad specificity for dNTPs and triphosphohydrolase-type hydrolysis. Acta Crystallographica Section D: Biological Crystallography, 2007, 63, 230-239.	2.5	27
104	Structure of the human Tim44 C-terminal domain in complex with pentaethylene glycol: ligand-bound form. Acta Crystallographica Section D: Biological Crystallography, 2007, 63, 1225-1234.	2.5	16
105	Crystallization and preliminary crystallographic analysis of molybdenum-cofactor biosynthesis protein C fromThermus thermophilus. Acta Crystallographica Section F: Structural Biology Communications, 2007, 63, 27-29.	0.7	4
106	Structure of the hypothetical protein PF0899 fromPyrococcus furiosusat 1.85â€Ã resolution. Acta Crystallographica Section F: Structural Biology Communications, 2007, 63, 549-552.	0.7	6
107	(NZ)CHO Contacts assist crystallization of a ParB-like nuclease. BMC Structural Biology, 2007, 7, 46.	2.3	17
108	Characterization of a corrinoid protein involved in the C1 metabolism of strict anaerobic bacterium Moorella thermoacetica. Proteins: Structure, Function and Bioinformatics, 2007, 67, 167-176.	2.6	28

Zнı-Jie Liu

#	Article	IF	CITATIONS
109	The multifunctional human p100 protein 'hooks' methylated ligands. Nature Structural and Molecular Biology, 2007, 14, 779-784.	8.2	72
110	Structural basis of CoA recognition by the Pyrococcus single-domain CoA-binding proteins. Journal of Structural and Functional Genomics, 2007, 7, 119-129.	1.2	3
111	Structural and transcriptional analyses of a purine nucleotide-binding protein from Pyrococcus furiosus: a component of a novel, membrane-bound multiprotein complex unique to this hyperthermophilic archaeon. Journal of Structural and Functional Genomics, 2007, 8, 1-10.	1.2	0
112	Crystal Structures of Tyrosyl-tRNA Synthetases from Archaea. Journal of Molecular Biology, 2006, 355, 395-408.	4.2	27
113	Crystal Structures of the Lytic Transglycosylase MltA from N.gonorrhoeae and E.coli: Insights into Interdomain Movements and Substrate Binding. Journal of Molecular Biology, 2006, 359, 122-136.	4.2	25
114	Crystal structure of obelin after Ca2+-triggered bioluminescence suggests neutral coelenteramide as the primary excited state. Proceedings of the National Academy of Sciences of the United States of America, 2006, 103, 2570-2575.	7.1	84
115	All three Ca2+-binding loops of photoproteins bind calcium ions: The crystal structures of calcium-loaded apo-aequorin and apo-obelin. Protein Science, 2005, 14, 663-675.	7.6	85
116	Life in the fast lane for protein crystallization and X-ray crystallography. Progress in Biophysics and Molecular Biology, 2005, 88, 359-386.	2.9	77
117	Protein Production and Crystallization at SECSG – An Overview. Journal of Structural and Functional Genomics, 2005, 6, 233-243.	1.2	14
118	A test of enhancing model accuracy in high-throughput crystallography. Journal of Structural and Functional Genomics, 2005, 6, 1-11.	1.2	45
119	Salvaging Pyrococcus furiosus Protein Targets at SECSG. Journal of Structural and Functional Genomics, 2005, 6, 121-127.	1.2	2
120	A non-natural dinucleotide containing an isomericL-related deoxynucleoside: dinucleotide inhibitors of anti-HIV integrase activity. Acta Crystallographica Section C: Crystal Structure Communications, 2005, 61, o518-o520.	0.4	1
121	On increasing protein-crystallization throughput for X-ray diffraction studies. Acta Crystallographica Section D: Biological Crystallography, 2005, 61, 123-129.	2.5	17
122	Parameter-space screening: a powerful tool for high-throughput crystal structure determination. Acta Crystallographica Section D: Biological Crystallography, 2005, 61, 520-527.	2.5	25
123	Away from the edge II: in-house Se-SAS phasing with chromium radiation. Acta Crystallographica Section D: Biological Crystallography, 2005, 61, 960-966.	2.5	10
124	The high-throughput protein-to-structure pipeline at SECSG. Acta Crystallographica Section D: Biological Crystallography, 2005, 61, 679-684.	2.5	22
125	Isolation, crystallization and preliminary X-ray analysis of a methanol-induced corrinoid protein fromMoorella thermoacetica. Acta Crystallographica Section F: Structural Biology Communications, 2005, 61, 537-540.	0.7	8
126	Three-dimesional structure of GlcNAcα1-4Gal releasing Endo-β-Galactosidase from Clostridium perfringens. Proteins: Structure, Function and Bioinformatics, 2005, 59, 141-144.	2.6	12

#	Article	IF	CITATIONS
127	Mechanism of Class 1 (Glycosylhydrolase Family 47) α-Mannosidases Involved in N-Glycan Processing and Endoplasmic Reticulum Quality Control. Journal of Biological Chemistry, 2005, 280, 16197-16207.	3.4	106
128	Structure of the Conserved Transcriptional Repressor Enhancer of Rudimentary Homologâ€,â€j. Biochemistry, 2005, 44, 5017-5023.	2.5	34
129	Crystal Structure of a Ca2+-discharged Photoprotein. Journal of Biological Chemistry, 2004, 279, 33647-33652.	3.4	51
130	Structure of Mouse Golgi α-Mannosidase IA Reveals the Molecular Basis for Substrate Specificity among Class 1 (Family 47 Glycosylhydrolase) α1,2-Mannosidases. Journal of Biological Chemistry, 2004, 279, 29774-29786.	3.4	48
131	Structural genomics ofPyrococcus furiosus: X-ray crystallography reveals 3D domain swapping in rubrerythrin. Proteins: Structure, Function and Bioinformatics, 2004, 57, 878-882.	2.6	18
132	Preparation and X-ray crystallographic analysis of the Ca2+-discharged photoprotein obelin. Acta Crystallographica Section D: Biological Crystallography, 2004, 60, 512-514.	2.5	7
133	Crystallization and preliminary X-ray analysis of GlcNAcα1,4Gal-releasing endo-β-galactosidase fromClostridium perfringens. Acta Crystallographica Section D: Biological Crystallography, 2004, 60, 537-538.	2.5	2
134	Displacement of iron by zinc at the diiron site of Desulfovibrio vulgaris rubrerythrin: X-ray crystal structure and anomalous scattering analysis. Journal of Inorganic Biochemistry, 2004, 98, 786-796.	3.5	19
135	X-ray Crystal Structure ofDesulfovibrio vulgarisRubrerythrin with Zinc Substituted into the [Fe(SCys)4] Site and Alternative Diiron Site Structuresâ€,‡. Biochemistry, 2004, 43, 3204-3213.	2.5	14
136	Structure determination of fibrillarin from the hyperthermophilic archaeon Pyrococcus furiosus. Biochemical and Biophysical Research Communications, 2004, 315, 726-732.	2.1	19
137	The Hyperthermophile Protein Sso10a is a Dimer of Winged Helix DNA-binding Domains Linked by an Antiparallel Coiled Coil Rod. Journal of Molecular Biology, 2004, 341, 73-91.	4.2	35
138	Crystallization and preliminary X-ray diffraction analysis of lectin-1 fromPseudomonas aeruginosa. Acta Crystallographica Section D: Biological Crystallography, 2003, 59, 1241-1242.	2.5	8
139	Atomic resolution structure of obelin: soaking with calcium enhances electron density of the second oxygen atom substituted at the C2-position of coelenterazine. Biochemical and Biophysical Research Communications, 2003, 311, 433-439.	2.1	56
140	Violet Bioluminescence and Fast Kinetics from W92F Obelin:Â Structure-Based Proposals for the Bioluminescence Triggering and the Identification of the Emitting Speciesâ€. Biochemistry, 2003, 42, 6013-6024.	2.5	57
141	Crystal Structure of the Cytoskeleton-associated Protein Glycine-rich (CAP-Gly) Domain. Journal of Biological Chemistry, 2002, 277, 48596-48601.	3.4	88
142	X-ray Crystal Structures of Reduced Rubrerythrin and Its Azide Adduct:Â A Structure-Based Mechanism for a Non-Heme Diiron Peroxidase. Journal of the American Chemical Society, 2002, 124, 9845-9855.	13.7	76
143	Structural basis for the emission of violet bioluminescence from a W92F obelin mutant. FEBS Letters, 2001, 506, 281-285.	2.8	44
144	Preparation and X-ray crystallographic analysis of recombinant obelin crystals diffracting to beyond 1.1â€Â Acta Crystallographica Section D: Biological Crystallography, 2001, 57, 1919-1921.	2.5	27

#	Article	IF	CITATIONS
145	Structures of an unliganded neurophysin and its vasopressin complex: Implications for binding and allosteric mechanisms. Protein Science, 2001, 10, 1869-1880.	7.6	42
146	The crystal structures of Phascolopsis gouldii wild type and L98Y methemerythrins: structural and functional alterations of the O2 binding pocket. Journal of Biological Inorganic Chemistry, 2001, 6, 418-429.	2.6	34
147	OBELIN CRYSTAL STRUCTURE: IMPLICATIONS FOR THE BIOLUMINESCENCE MECHANISM. , 2001, , .		0
148	Structure of the Ca <sup>2+</sup> â€regulated photoprotein obelin at 1.7 à resolution determined directly from its sulfur substructure. Protein Science, 2000, 9, 2085-2093.	7.6	170
149	Low-salt crystallization of T7 RNA polymerase: a first step towards the transcription bubble complex. Acta Crystallographica Section D: Biological Crystallography, 1999, 55, 1188-1192.	2.5	2
150	Preparation and preliminary study of crystals of the recombinant calcium-regulated photoprotein obelin from the bioluminescent hydroid Obelia longissima. Acta Crystallographica Section D: Biological Crystallography, 1999, 55, 1965-1966.	2.5	5
151	Aldehyde Dehydrogenase Catalytic Mechanism. Advances in Experimental Medicine and Biology, 1999, 463, 53-59.	1.6	47
152	The first structure of an aldehyde dehydrogenase reveals novel interactions between NAD and the Rossmann fold. Nature Structural Biology, 1997, 4, 317-326.	9.7	289
153	Crystal Structure of a Class 3 Aldehyde Dehydrogenase at 2.6Ã Resolution. Advances in Experimental Medicine and Biology, 1996, 414, 1-7.	1.6	12
154	Conserved Residues in the Aldehyde Dehydrogenase Family. Advances in Experimental Medicine and Biology, 1996, 414, 9-13.	1.6	12
155	Procedure for reductive methylation of protein to improve crystallizability. Protocol Exchange, 0, , .	0.3	9